Journal of Ginseng Research 47 (2023) 65–73

Contents lists available at ScienceDirect

Journal of Ginseng Research

journal homepage: https://www.sciencedirect.com/journal/journal-of-ginseng-research

Research Article

Protective effects of *Panax ginseng* berry extract on blue light-induced retinal damage in ARPE-19 cells and mouse retina

Hye Mi Cho [a], Sang Jun Lee [b], Se-Young Choung [a, c, *]

[a] Department of Biomedical and Pharmaceutical Sciences, Graduate School, Kyung Hee University, Seoul, Republic of Korea
[b] Holistic Bio CO., Seongnam, Republic of Korea
[c] Department of Preventive Pharmacy and Toxicology, College of Pharmacy, Kyung Hee University, Seoul, Republic of Korea

ARTICLE INFO

Article history:
Received 1 November 2021
Received in revised form
30 March 2022
Accepted 11 April 2022
Available online 18 April 2022

Keywords:
Panax ginseng berry
Age-related macular degeneration
Blue light exposure
A2E
ARPE-19 cells

ABSTRACT

Background: Age-related macular degeneration (AMD) is a significant visual disease that induces impaired vision and irreversible blindness in the elderly. However, the effects of *ginseng* berry extract (GBE) on the retina have not been studied. Therefore, this study aimed to investigate the protective effects of GBE on blue light (BL)-induced retinal damage and elucidate its underlying mechanisms in human retinal pigment epithelial cells (ARPE-19 cells) and Balb/c retina.

Methods: To investigate the effects and underlying mechanisms of GBE on retinal damage *in vitro*, we performed cell viability assay, pre-and post-treatment of sample, reactive oxygen species (ROS) assay, quantitative real-time PCR (qRT-PCR), and western immunoblotting using A2E-laden ARPE-19 cells with BL exposure. In addition, Balb/c mice were irradiated with BL to induce retinal degeneration and orally administrated with GBE (50, 100, 200 mg/kg). Using the harvested retina, we performed histological analysis (thickness of retinal layers), qRT-PCR, and western immunoblotting to elucidate the effects and mechanisms of GBE against retinal damage *in vivo*.

Results: GBE significantly inhibited BL-induced cell damage in ARPE-19 cells by activating the SIRT1/PGC-1α pathway, regulating NF-kB translocation, caspase 3 activation, PARP cleavage, expressions of apoptosis-related factors (BAX/BCL-2, LC3-II, and p62), and ROS production. Furthermore, GBE prevented BL-induced retinal degeneration by restoring the thickness of retinal layers and suppressed inflammation and apoptosis via regulation of NF-kB and SIRT1/PGC-1α pathway, cleavage of caspase 3 and PARP, and expressions of apoptosis-related factors *in vivo*.

Conclusions: GBE could be a potential agent to prevent dry AMD and progression to wet AMD.

1. Introduction

Age-related macular degeneration (AMD) is a degenerative eye disease that is a leading cause of visual disorder and irreversible blindness in the elderly. The AMD is categorized into two forms: dry AMD and wet AMD. Dry AMD is characterized by accumulating extracellular yellowish deposits called drusen and can progress to wet AMD [1,2]. Wet AMD is associated with the growth of abnormal new vessels from the choroid. Choroidal neovascularization leads to leakage of fluids and blood, also causes severe vision loss. Injection of anti-VEGF antibody is a standard treatment for wet AMD [3,4]. However, there is no effective treatment that could prevent dry AMD or progression to wet AMD.

Retinal pigment epithelial (RPE) cells play a significant role in maintaining the photoreceptor in the macular [5]. The RPE cells phagocytose the outer segments of the photoreceptor. RPE lipofuscin is a byproduct of the phagocytosed photoreceptor outer segment [6]. The major fluorophore of the RPE lipofuscin is *N*-retinylidene-*N*-retinylethanolamine (A2E), which is associated with the onset of AMD by accumulating in RPE cells with age [7]. When A2E is exposed to light, including blue light (BL), it is oxidized to oxo-A2E and contributes to the RPE cell damage because reactive oxygen species (ROS) are produced and cause oxidative stress, inflammation, and apoptosis [8,9]. In addition, the risk factors for developing AMD include age, gender, obesity, hypertension, genetics, smoking, and sunlight exposure. Among them, A2E accumulation and exposure to BL are the critical factors for AMD

* Corresponding author. Department of Biomedical and Pharmaceutical Sciences, Graduate School, Kyung Hee University, 26, Kyungheedae-ro, Dongdaemun-gu, Seoul, 02447, Republic of Korea.
E-mail address: sychoung@khu.ac.kr (S.-Y. Choung).

https://doi.org/10.1016/j.jgr.2022.04.002

Abbreviations

AMD	age-related macular degeneration
RPE	retinal pigmented epithelial
A2E	*N*-retinylidene-*N*-retinylethanolamine
GBE	*ginseng* berry extract
BL	blue light
ROS	reactive oxygen species

development [10,11]. Some *in vitro* studies have reported that BL exposure induces RPE cell death with A2E concentration-dependently. Also, the RPE cell death was maximal at wavelengths ranging from 415 to 455 nm (blue light) [10]. Therefore, BL is a critical ray among visible light contributing to RPE cell apoptosis and the development of AMD. Furthermore, some *in vivo* studies have demonstrated that BL exposure induced oxidative stress, inflammation, and angiogenesis, leading to retinal degeneration [12,13]. In addition, BL exposure causes photoreceptor degeneration and apoptosis, decreasing the thickness of the outer nuclear layer (ONL) in the retina [14]. Thus, a preventive approach for dry AMD is focused on the preservation of RPE by photo-oxidation.

Panax ginseng berry is a fruit of *Panax ginseng* used as a medicinal plant traditionally in Asia [15]. It has various biological effects such as anti-inflammatory, anti-oxidative, neuroprotective, anti-cancer, and anti-diabetic activities [16–19]. The *Panax ginseng* berry extract (GBE) contains significant amounts of ginsenosides, phenolic compounds (chlorogenic acid, gentisic acid, and rutin), and polysaccharides [20–22]. Among them, the most abundant compound of GBE is ginsenoside Re, and it is 30–40 times more than that of ginseng root [16]. Previous studies have reported that ginsenosides Rb1, Rd, and Rg1 from ginseng root inhibit ROS production [23,24] and apoptosis in RPE cells [23]. However, the protective effects of GBE on the retina have not been demonstrated both *in vitro* and *in vivo*. Accordingly, we hypothesized that GBE would have protective effects on BL-induced damage in A2E-laden RPE cells and retinal degeneration in mice. Furthermore, we aimed to investigate the underlying mechanisms of GBE on retinal damage *in vitro* and *in vivo*. Finally, we confirmed that ginsenoside Re would be an active compound of GBE on retinal degeneration through *in vitro* experiments.

2. Materials and methods

2.1. Preparation of GBE and ginsenoside Re

Panax ginseng berry (Panax ginseng Meyer) extract was obtained from Holistic Bio Corporation (Gyeonggi-do, Republic of Korea). Panax ginseng berry was washed with water, and the seeds were removed. The remaining pulp and rinds were collected. One hundred percent water extraction was performed under reflux conditions for 2–5 h. The extract was then filtered and evaporated. The extract solution was spray-dried to obtain a powder state of GBE and stored at −20 °C until use. The extraction yield of GBE is 2.5%.

Each pulverized GBE (600 mg) was extracted with 6 mL of 70% methanol using a Retsch MM400 mixer mill (Retsch GmbH, Haan, Germany), operated at 30 Hz/s for 10 min. Subsequently, the samples were subjected to sonication in an ultrasonic water bath (Power Sonic 305; Hwashin Technology Co., Seoul, Korea) for 5 min and centrifuged at 17,000 rpm at 4 °C for 15 min. The supernatant was filtered using a 0.2-mm polytetrafluoroethylene filter and concentrated using a speed vacuum concentrator (Modulspin 31; Biotron, Incheon, Korea). The samples collected finally were weighed and reconstituted in 70% methanol. The final concentration of the samples was 50 mg/mL for ultrahigh performance liquid chromatography-electrospray ionization-tandem mass spectrometry (UHPLC-ESI-MS/MS) analysis.

2.2. Cell culture

Human RPE cells (ARPE-19 cells) were obtained from American Type Culture Collection (Manassas, VA, USA). The cells were cultured in Dulbecco's modified Eagle's medium F-12 (Welgene, Daegu, Republic of Korea). The medium was supplemented with 10% fetal bovine serum (FBS) and 1% penicillin-streptomycin. ARPE-19 cells were maintained at 37 °C in a humidified atmosphere containing 5% CO_2.

2.3. Blue light illumination and cell viability assay

The ARPE-19 cells were seeded at a density of 5×10^5 cells/well in 6-well plates and then maintained in the medium for 48 h. The cells were treated with 20 μM of A2E for three times (day 1, 3, 5) in 6 days and then treated with GBE (80 μg/mL) or lutein (30 μM) twice (day 7, 9) in 4 days. 30 μM of lutein was used as the positive control. Subsequently, the media were replaced with PBS, and the cells were irradiated with BL (430 nm, 6000 lux) for 20 min on day 11 and incubated for an additional 6 h.

The cell viability of the GBE and A2E in ARPE-19 cells was determined by the Cell Count Kit-8 (CCK) assay (Dojindo Labs., Kumamoto, Japan). The ARPE-19 cells were seeded in a 96-well culture plate and treated with GBE (20, 40, 80, 160, 320, 640, 1280 μg/mL) or A2E (5, 10, 20, 40, 60 μM) or ginsenoside Re (1, 2, 4, 8, 16 μM) for 24 h. After adding 10 μL of the CCK-8 solution to each well, the cells were incubated for 1 h at 37 °C. Absorbance at 450 nm was measured using the ELISA reader (Bio-Tek instrument: Power Wave XS microplate spectrophotometer, Winooski, VT, USA). To measure the cytotoxicity of BL in A2E-laden RPE cells, the cells were treated with A2E at concentrations of 0, 5, 10, 20, 40, and 60 μM for 24 h. After that, the cells were exposed to BL (430 nm, 6000 lux, 10 min). After the incubation for 24 h, the cell viability was determined by CCK assay.

2.4. Pre & post-treatment of GBE with BL illumination

ARPE-19 cells were seeded in 96-well plates at a density of 1.5×10^4 cells per well and maintained for 24 h. Pre-treatment system: the ARPE-19 cells were treated with GBE (40, 80, 160 μg/mL) or lutein (30 μM) or ginsenoside Re (4, 8 μM) for 24 h. After the supernatant was removed, the cells were treated with A2E at 20 μM for 24 h. Post-treatment system: the cells were incubated with A2E at 20 μM for 24 h. After the supernatant was suctioned, the cells were treated with GBE or lutein or ginsenoside Re at the designated concentration for 24 h. In both treatment systems, the media was removed and replaced with PBS. Then, the cells were illuminated with BL (430 nm, 6000 lux, 10 min), except for the control. After the cells were incubated with the medium for 24 h, the cell viability was assessed using CCK assay.

2.5. Quantitative analysis of cellular reactive oxygen species (ROS)

After the treated ARPE-19 cells were exposed to BL and incubated for 6 h, the cells were harvested for ROS quantification using OxiSelect *in vitro* ROS/RNS assay kit (Cell Biolabs, SanDiego, CA, USA). According to the manufacturer's instruction, the cells were suspended in PBS and sonicated on ice. Then, the cells were

centrifuged at 10,000 g for 5 min at 4 °C. The obtained supernatant was added with dichlorofluorescin (DCFH) solution in a 96-well plate for 30 min at room temperature. The fluorescence intensity of DCF was determined using the fluorescence microplate reader (FLUOstar Omega, BMG Labtech, Cary, NC) at 480 nm excitation and 530 nm emission.

2.6. Animals and experimental design

Balb/c male mice aged 5 weeks were purchased from DBL (Cheongju, Republic of Korea). The mice were housed in standard cages and maintained with a 12:12 h light-dark cycle at 25 ± 1 °C. The mice were fed with a standard laboratory diet (Central Lab Animal, Seoul, Republic of Korea) and water ad libitum. All experiments with mice were conducted according to the ARVO guidelines and protocols approved by the Institutional Animal Care and Use Committee guideline of Kyung Hee University [KHSASP-20-439].

The mice were randomly divided into six groups (10 mice in each group). Normal control group: animals administered with vehicle (0.5% carboxyl methylcellulose, CMC). Vehicle-treated group: animals exposed to BL and administered with vehicle. Reference control group: animals exposed to BL with administration of lutein (50 mg/kg body weight). Experimental groups: animals exposed to BL with administration of GBE (three groups, individually 50, 100, 200 mg/kg body weight).

2.7. Sample administration and BL exposure

The sample administration and BL exposure were performed in accordance with the schedules in our previous study [25]. Before BL exposure to mice, lutein (50 mg/kg) or GBE (50, 100, 200 mg/kg) was orally administered every 24 h for 5 days. After dark acclimation for 24 h, sample administration and BL exposure were performed every 24 h for 14 days. The reference control and experimental groups were administered lutein or GBE via gastric intubation. One hour after the administration, the mice except for the normal control group were exposed to BL (430 nm, 10,000 lux) for 1 h. After the last administration and BL exposure, all the mice were maintained in dark cages for 24 h and were euthanized using a CO_2 chamber.

2.8. Histological analysis

Each eye was enucleated, and the eyeballs were fixed in Davidson's solution (10% neutral buffered formaldehyde: 95% ethanol: glacial acetic acid: distilled water = 1:3:1:3) for 7 days.

The entire eyes were embedded in paraffin and were cut along the vertical meridian of eyeballs. Paraffin-embedded sections (3 μm thickness) were stained with hematoxylin and eosin (H&E) and photographed using an optical microscope (Olympus Optical, Tokyo, Japan). The thickness of the outer nuclear layer (ONL), inner nuclear layer (INL), photoreceptor layer (PL), and the whole retina was measured between 600 and 900 μm from the optic nerve at 60 μm intervals using Image J software (National Institutes of Health, Bethesda, MD, USA). The data from 6 locations were averaged for each eye.

2.9. Quantitative real-time PCR (qRT-PCR)

Total RNA from the treated ARPE-19 cells and retinas was extracted using easy-RED™ (iNtRON biotechnology, Seongnam, Republic of Korea). cDNA was synthesized using a PrimeScript™ 1st strand cDNA synthesis kit (TaKaRa, Shiga, Japan). qRT-PCR was conducted by an ABI StepOnePlus™Real-Time PCR System (Applied Biosystems, Foster City, CA, USA) using SYBR Premix Ex Tag (TaKaRa, Shiga, Japan). The primer sequences for qRT-PCR were listed in Supplementary Table 1. The mRNA expression levels were normalized relative to GAPDH.

2.10. Western immunoblotting

ARPE-19 cells and retinal tissues were lysed in lysis buffer containing cOmplete™ Protease Inhibitor Cocktail tablets and PhosSTOP™ (Roche Diagnostics, Indianapolis, IN, USA). The lysates were sonicated for 20 min, dispersed, and centrifuged at 10,000 g for 20 min at 4 °C. Nuclear and cytosol fractions of the protein were obtained separately by a Nuclear Extraction Kit (Abcam, Cambridge, MA, USA) according to the manufacturer's instructions (Cat No: ab113474). Primary antibodies against NF-kB p65 and IkB-alpha were obtained from Santa Cruz Biotechnology (Santa Cruz, CA, USA), PARP, caspase 3, cleaved caspase 3, SirT1, LC3B, and p62 were obtained from Cell Signaling Technology (Danvers, MA, USA), and PGC-1 alpha was obtained from Abcam (Cambridge, MA, USA). The membranes were incubated with horseradish peroxidase (HRP) - conjugated secondary antibodies for 2 h at 1 : 5000 dilution in blocking solution. The protein expression levels were normalized to β-actin (Santa Cruz, CA, USA) and Lamin B1 (Cell Signaling Technology, Danvers, MA, USA). The bands were visualized using a LAS3000 Luminescent image analyzer (Fuji Film, Tokyo, Japan). The protein bands were quantified using Image J software (National Institute of Health, Bethesda, MD, USA).

2.11. Statistical analysis

Shapiro-Wilk test was conducted to analyze the normality of data. Normally distributed data included cell viability tests, pre-/post-treatment tests, and thickness of the retinal layers. The normal distribution data were analyzed via one-way ANOVA followed by Tukey's post hoc tests. Mann-Whitney test was used to analyze the non-normally distributed data. Significant differences were assessed using SPSS version 25 statistical software (Chicago, IL, USA).

3. Results and discussion

3.1. GBE is profiled by UHPLC-ESI-MS/MS

The UHPLC-ESI-MS/MS analysis of GBE was performed to identify the main compound of GBE in Supplementary Fig. S1 [26]. We confirmed that the highest peak was identified as ginsenoside Re. The content of ginsenoside Re in GBE was determined using HPLC-UV method [27]. GBE was standardized to contain 5% of ginsenoside Re.

3.2. GBE inhibits cell death induced by A2E treatment and blue light exposure in ARPE-19 cells

A2E is photo-oxidized by light exposure, especially BL, contributing to cell damage. Our previous study demonstrated that A2E did not show cytotoxicity up to 20 μM, but BL exposure reduced cell viability in ARPE-19 cells treated with 20 μM A2E [28]. We estimated the cytotoxicity of GBE and A2E in ARPE-19 cells. GBE and A2E did not show cytotoxicity up to 160 μg/mL and 20 μM, respectively (Fig. 1A and B). Cell viability was reduced by 47.8% when treated with 20 μM A2E and irradiated with BL (Fig. 1C). Thus, we selected 20 μM A2E for the following experiments. The pre-and post-treatment of GBE inhibited BL-induced cell death in a concentration-dependent manner (Fig. 1D and E). These results suggest that GBE protects the RPE cells against cell death induced by BL exposure. Based on the efficacy experiments with a variable

concentration of GBE, we selected GBE at a concentration of 80 μg/mL for subsequent mechanism studies.

3.3. GBE activates SIRT1/PGC-1α signaling pathway and inhibits BL induced inflammatory response in A2E-laden ARPE-19 cells

Oxidative stress is closely related to the onset and progression of AMD and is induced by the generation of excess ROS, which is mainly produced in mitochondria [29]. Also, oxidative stress caused by BL exposure leads to inflammation that contributes to AMD. Recent studies demonstrated that the SIRT1 signaling pathway modulates the inflammatory response by regulating NF-kB transcriptional activity through deacetylation of NF-kB p65 [30]. The SIRT1 is induced under mild oxidative stress as a compensatory response. However, the level of SIRT1 is decreased by the increasing degradation of SIRT1 under severe or prolonged oxidative stress conditions. SIRT1 is critical to regulating cellular redox homeostasis as well as inflammation [31]. SIRT1 regulates the activation of PGC-1α, which is a master regulator of mitochondrial biogenesis. PGC-1α modulates the expressions of antioxidant enzymes such as SOD2, thus, contributing to the control of ROS production and mitochondrial redox homeostasis [29]. BL exposure increased the gene and protein levels of SIRT1 and PGC-1α in A2E-laden ARPE-19 cells (Fig. 2A and D). Treatment of GBE significantly upregulated the gene and protein levels of SIRT1 and PGC-1α compared to the BL exposed group. Recent studies reported that A2E treatment induced the gene expression of PGC-1α in ARPE cells [32]. The gene expression of *TFAM*, a mitochondrial transcription factor and target of PGC-1α, is slightly induced after BL exposure and enhanced by 92% in the GBE treatment group (Fig. 2A). It was reported that mRNA expression of *TFAM* was upregulated by A2E in RPE cells [32]. BL illumination decreased the gene expression of *SOD2*, which serves as scavenging the excess mitochondrial ROS, while the expression was increased by 100% in the GBE treatment group (Fig. 2B). These findings indicate that GBE activates SIRT1/PGC-1α signaling pathway in the RPE cells. Our study also demonstrates that BL exposure upregulates the gene and protein levels of SIRT1 and PGC-1α as a compensatory response against mild oxidative stress in A2E-laden ARPE-19 cells.

ROS induced the activation of the NF-kB pathway, contributing to the inflammatory response. NF-kB is a transcription factor that is bound to IkB-α in the cytosol. When a variety of stimuli occurs, including light irradiation, IkB-α is degraded. Then NF-kB separated from IkB-α is translocated from the cytosol to the nucleus, leading to the gene expressions involved in inflammation such as *IL-1β*, *IL-6*, and *MCP-1* in ARPE-19 cells [33–35]. The protein level of IkB-α was decreased by 47% and the nuclear protein level of NF-kB was increased by 248% in the BL-exposed group compared to the normal group (Fig. 2E). In Fig. 2C, BL exposure upregulated the gene expressions of inflammation-related factors (IL-1beta, IL-6, MCP-1, and CXCL-2) and angiogenesis factor (VEGF-alpha) in ARPE-19 cells. Treatment of GBE elevated the protein level of IkB-α by 55%, decreasing the nuclear protein level of NF-kB by 41%, resulting in significantly reducing gene expressions related to inflammation more than lutein did. These results suggest that GBE treatment inhibits BL-induced inflammation by attenuating IkB-α degradation and NF-kB translocation in ARPE-19 cells. GBE also regulates the NF-kB pathway by activating the SIRT1/PGC-1α signaling pathway in the cells.

3.4. GBE inhibits apoptosis and restores the inhibition of autophagic flux induced by BL exposure in A2E-laden ARPE-19 cells

Previous studies demonstrated that BL exposure induced photooxidation of A2E, leading to increase ROS generation and apoptotic cell death in A2E-laden ARPE-19 cells [28,34]. BL illumination

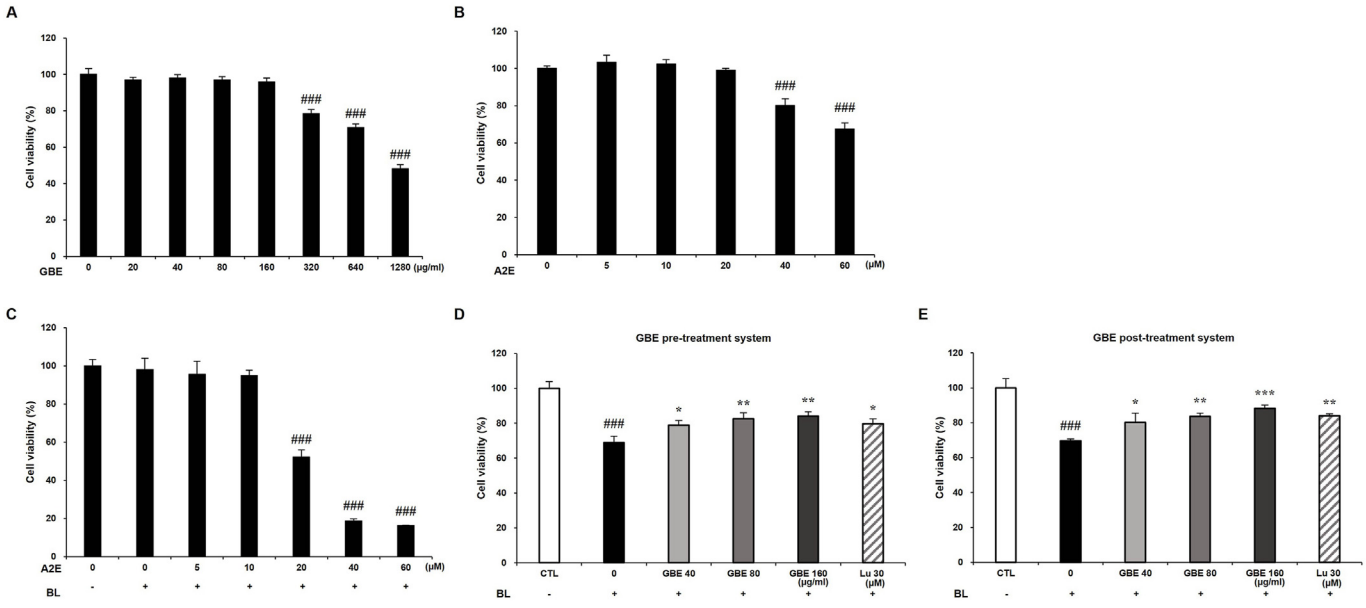

Fig. 1. GBE inhibits cell death induced by A2E treatment and blue light exposure in ARPE-19 cells. (A) Cell viability of GBE in ARPE-19 cells was measured using CCK assay. The results were presented as the mean ± SD (n = 4) of three independent experiments. ###p < 0.001 vs. the untreated control. (B) Cell viability of A2E in ARPE-19 cells was measured using CCK assay. The results were presented as the mean ± SD (n = 5) of three independent experiments. ###p < 0.001 vs. the untreated control. (C) ARPE-19 cells were treated with A2E at the concentrations of 0, 5, 10, 20, 40, 60 μM and incubated for 24 h. After blue light (6000 lux) exposure for 10 min, cell viability was measured by the CCK assay. (D) ARPE-19 cells were incubated with GBE (0–160 μg/mL) or lutein (30 μM) for 24 h. Then, the RPE cells were treated with A2E at 20 μM for 24 h. After the cells were irradiated with blue light (6000 lux) for 10 min and then incubated for 24 h, cell viability was measured by the CCK assay. (E) ARPE-19 cells were treated with A2E at 20 μM for 24 h. Then, the RPE cells were incubated with GBE (0–160 μg/mL) or lutein (30 μM) for 24 h. After the cells were irradiated with blue light (6000 lux) for 10 min and then incubated for 24 h, cell viability was measured by the CCK assay. The results were presented as mean ± SD (n = 3) of three independent experiments. ###p < 0.001 vs. the untreated control. *p < 0.05, **p < 0.01, ***p < 0.001 vs. blue light only treated group.

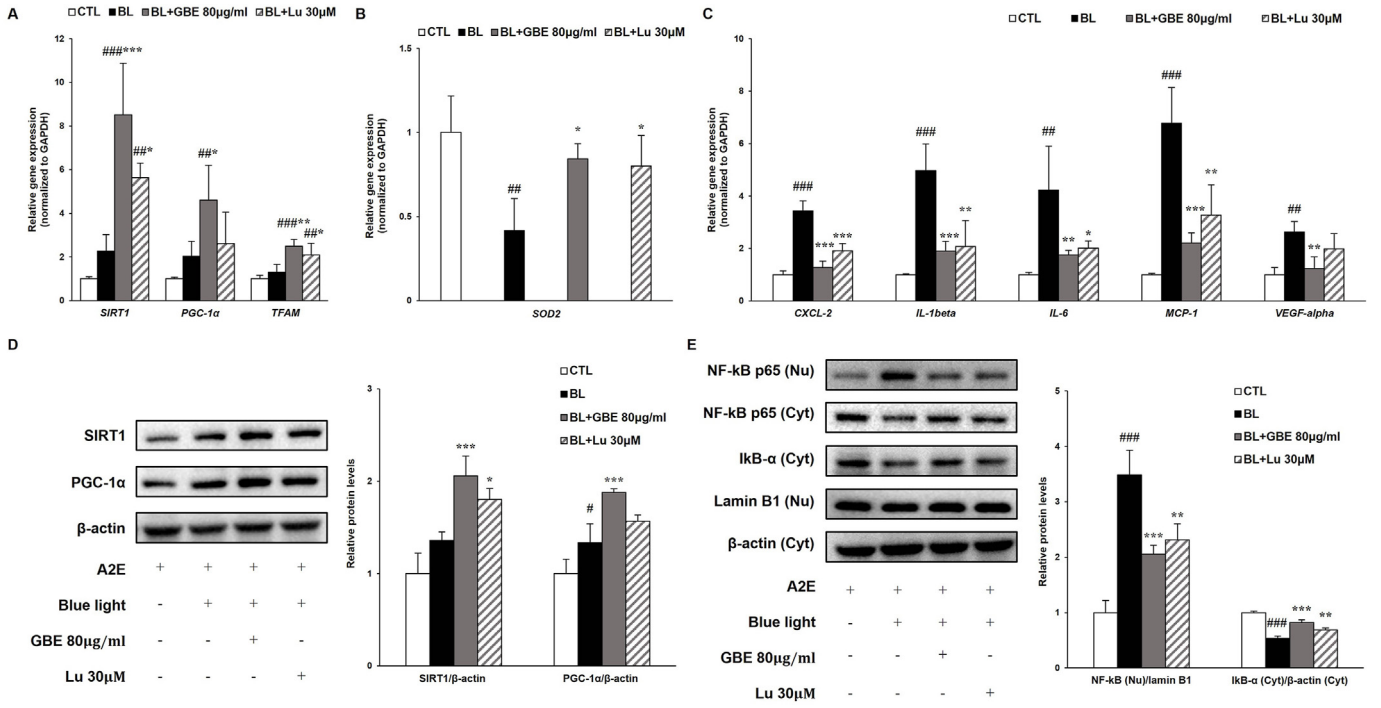

Fig. 2. GBE activates SIRT1/PGC-1α signaling pathway and inhibits BL induced inflammatory response in A2E-laden ARPE-19 cells. (A) Gene expressions of *SIRT1*, *PGC-1α*, and *TFAM* were analyzed by quantitative real time PCR in A2E-laden ARPE-19 cells. (B) Gene expression of *SOD2* was measured by quantitative RT-PCR in A2E-laden ARPE-19 cells. (C) Gene expressions of inflammation-related factors (CXCL-2, IL-1beta, IL-6, MCP-1, and VEGF-alpha) were measured by qRT-PCR and normalized to GAPDH. (D) Protein levels of SIRT1 (120 kDa) and PGC-1α (92 kDa) were detected in A2E-laden ARPE-19 cells by western immunoblotting. (E) Protein levels of NF-kB p65 (65 kDa) were measured in nucleus and cytosol fractions. IkBα (37 kDa) was detected in cytosol fraction. Protein levels of NF-kB and IkBα were quantified by band density. The results were presented as mean ± SD (n = 4) of three independent experiments. $^{\#}p < 0.05$, $^{\#\#}p < 0.01$, $^{\#\#\#}p < 0.001$ vs. CTL, $^{*}p < 0.05$, $^{**}p < 0.01$, $^{***}p < 0.001$ vs. BL.

significantly increased total ROS/RNS level, while concentration-dependently decreased by GBE (Fig. 3A). BL illumination increased the ratio of *BAX/BCL-2*, suggesting increased mitochondrial apoptosis (Fig. 3B). However, the ratio was considerably attenuated by 58% in the GBE treatment group compared to the BL-exposed group. BAX, a pro-apoptotic protein, causes the release of cytochrome *c* from mitochondria, leading to the activation of caspase 3 [36]. Cleaved caspase 3, an activated form of caspase 3, induces cleavage of PARP, which is a marker of apoptosis [37]. Cleavage of caspase 3 and PARP was increased by BL exposure and significantly reduced by 36% and 39% in the GBE treatment group, respectively (Fig. 3C). A recent study reported that BL exposure in A2E-laden ARPE-19 cells increased LC3-II and p62 protein levels, indicating inhibition of autophagy [38]. Inhibition of autophagy increases activation of caspase 3, contributing to apoptotic RPE cell death. p62, a marker of autophagic flux, is degraded and decreased as autophagy progresses [39,40]. In Fig. 3C, the protein levels of LC3-II and p62 were increased when exposed to BL in A2E-laden ARPE-19 cells. However, the elevation of both protein levels was attenuated by 35% and 26% in the GBE treatment group, respectively, suggesting that GBE restored the inhibition of autophagic flux by BL exposure in A2E-laden ARPE-19 cells. The previous study reported that impaired autophagy by A2E photo-oxidation caused the autophagic clearance to fail, leading to RPE damage and onset of AMD [38]. However, we still need to investigate further to clarify the underlying mechanisms of GBE on autophagy.

3.5. GBE protects BL-induced retinal degeneration in retina

GBE exerted protective effects on BL-induced retinal damage *in vitro*. To investigate the efficacy of GBE on retinal degeneration in mice, we performed histological analysis using our established animal model [25]. Each eye was enucleated and histological analyses were performed after oral administration of GBE and BL exposure to mice for 14 days every 24 h. In Fig. 4 A, representative retina images are shown between 600 and 900 μm from the optic nerve. We measured the thickness of the whole retina, ONL, INL, and PL of six groups (Normal, BL, BL + GBE 50/100/200 mg/kg, BL + Lu 50 mg/kg). The thicknesses of the whole retina, ONL, INL, and PL were considerably decreased in the vehicle-treated group compared to the normal control group (Fig. 4B). However, the administration of GBE dose-dependently restored the thickness of all the layers. This indicates that the administration of GBE protects against retinal degeneration induced by BL irradiation.

3.6. GBE activates SIRT1/PGC-1α signaling pathway and inhibits BL induced inflammatory response in retina

We found that GBE inhibited inflammation by activating the SIRT1/PGC-1α signaling pathway in ARPE-19 cells. Based on these findings, we investigated the action mechanisms of GBE in the mouse retina, focusing on the SIRT1/PGC-1α pathway and inflammatory response. BL irradiation downregulated the gene and protein levels of SIRT1 and PGC-1α in the retina (Fig. 5A and D). However, the administration of GBE significantly increased the levels of SIRT1 and PGC-1α. The gene expressions of *Tfam* and *Sod2*, which were decreased after BL exposure, were increased by 71% and 165% in the GBE administration group, respectively (Fig. 5A and B). These findings suggest that GBE activated SIRT1/PGC-1α signaling pathway in the retina. We firstly demonstrated that BL illumination downregulated SIRT1, PGC-1α, and *Tfam* expressions in the retina. On the other hand, their expressions were upregulated by BL exposure in our *in vitro* study. The difference between the *in vitro* and *in vivo* studies could be explained by the induction

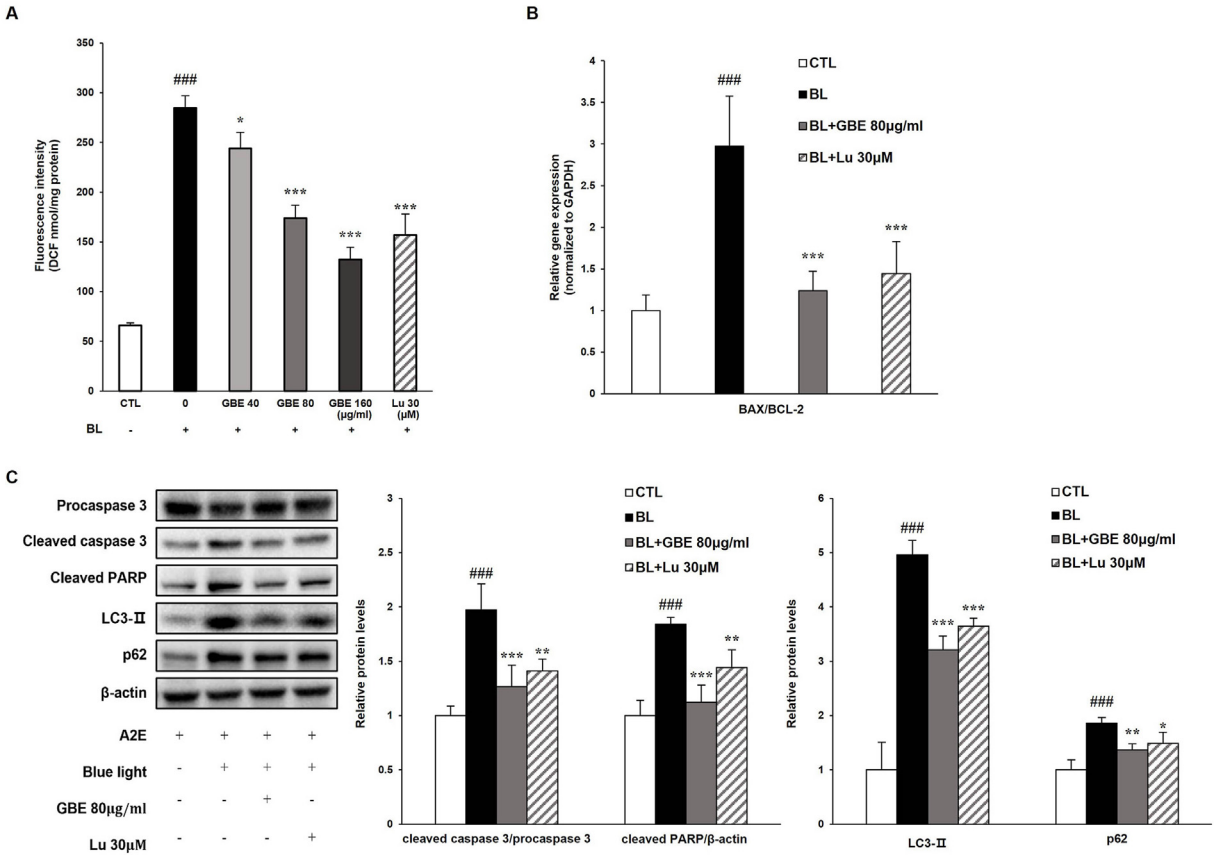

Fig. 3. GBE inhibits apoptosis and restores the inhibition of autophagic flux induced by BL exposure in A2E-laden ARPE-19 cells. (A) Quantification of ROS/RNS was analyzed in A2E-laden ARPE-19 cells. The results were presented as mean ± SD (n = 3) of three independent experiments. $^{###}p < 0.001$ vs. CTL. $^{*}p < 0.05$, $^{***}p < 0.001$ vs. blue light only treated group. (B) Gene expressions of apoptosis-related factors (BAX/BCL-2) were detected in A2E-laden ARPE-19 cells by qRT-PCR and normalized to GAPDH. (C) Protein levels of procaspase 3 (35 kDa), cleaved caspase 3 (17 kDa), cleaved PARP (89 kDa), LC3-II (14 kDa), and p62 (62 kDa) were measured by western immunoblotting and quantified by band density. The results were presented as mean ± SD (n = 4) of three independent experiments. $^{###}p < 0.001$ vs. CTL, $^{*}p < 0.05$, $^{**}p < 0.01$, $^{***}p < 0.001$ vs. BL.

of SIRT1 under mild oxidative stress, like our *in vitro* experimental conditions. However, SIRT1 was degraded and reduced under severe or prolonged oxidative stress, such as our *in vivo* conditions [31].

Previous studies reported that the SIRT1 pathway regulated inflammation by modulating NF-kB activation [30]. We found that BL exposure increased the translocation of NF-kB into the nucleus, followed by upregulation of the expressions of inflammatory-related genes (*IL-1beta*, *IL-6*, *MCP-1*, and *CXCL-2*) and *VEGF-alpha* in ARPE-19 cells. To correlate with *in vitro* studies, the expression levels of inflammation-related genes (*Tnf-alpha, Cxcl-2, Mcp-1, IL-1beta,* and *IL-6*), proteins (NF-kB and IkB-α), and angiogenesis-related genes (*Mmp-2*, *Mmp-9*, and *Vegf-alpha*) were analyzed in the retina (Fig. 5C and E). BL exposure activated the NF-kB translocation, causing the transcription of those genes in the retina. The GBE administration attenuated the expressions of genes related to inflammation and angiogenesis by inhibiting IkB-α degradation and NF-kB translocation. Especially, the expression of *Vegf-alpha* was significantly reduced by 64% in the GBE administration group, indicating that GBE prevented the advancement to wet AMD. We suggest that GBE suppresses inflammation by activating SIRT1/PGC-1α pathway and regulating the NF-kB pathway in the retina.

3.7. GBE inhibits apoptosis and restores the inhibition of autophagic flux induced by BL exposure in the retina

In this study, GBE inhibited apoptosis by attenuating the upregulation of the *BAX/BCL-2* ratio and autophagy inhibition in ARPE-19 cells. To correlate with *in vitro* studies, we examined gene and protein levels on the apoptotic pathway in the retina. The ratio of *Bax/Bcl-2* was elevated in the BL-exposed group, followed by upregulation of the protein levels of cleaved caspase 3 and cleaved PARP (Fig. 6A and B). The administration of GBE significantly decreased the *Bax/Bcl-2* ratio by 74% and cleaved caspase 3 and cleaved PARP protein levels by 42% and 29%, respectively. Recent studies reported that autophagy played a crucial role in regulating drusen formation and AMD pathogenesis. Also, autophagy was suppressed by exposure to chronic oxidative stress [41,42]. BL exposure increased the LC3-II and p62 protein levels, while GBE administration considerably reduced their levels by 36% and 26%, respectively (Fig. 6A and B). These results indicate that GBE administration prevents apoptosis and inhibition of autophagic flux in the retina. Furthermore, GBE administration has more protective effects than lutein in the retina. Considering that lutein is widely used in clinical trial [43], GBE could be potentially used in the clinical trial for retina protection.

3.8. Ginsenoside Re is an active component of GBE on retinal degeneration

To investigate whether ginsenoside Re, the most abundant compound in GBE, was effective on retinal degeneration, we evaluated its efficacy using pre-and post-treatment systems. We measured the cytotoxicity of ginsenoside Re to examine its efficacy within non-toxic concentrations. Ginsenoside Re didn't show cytotoxicity up to 16 μM in RPE cells (Supplementary Fig. S2). In

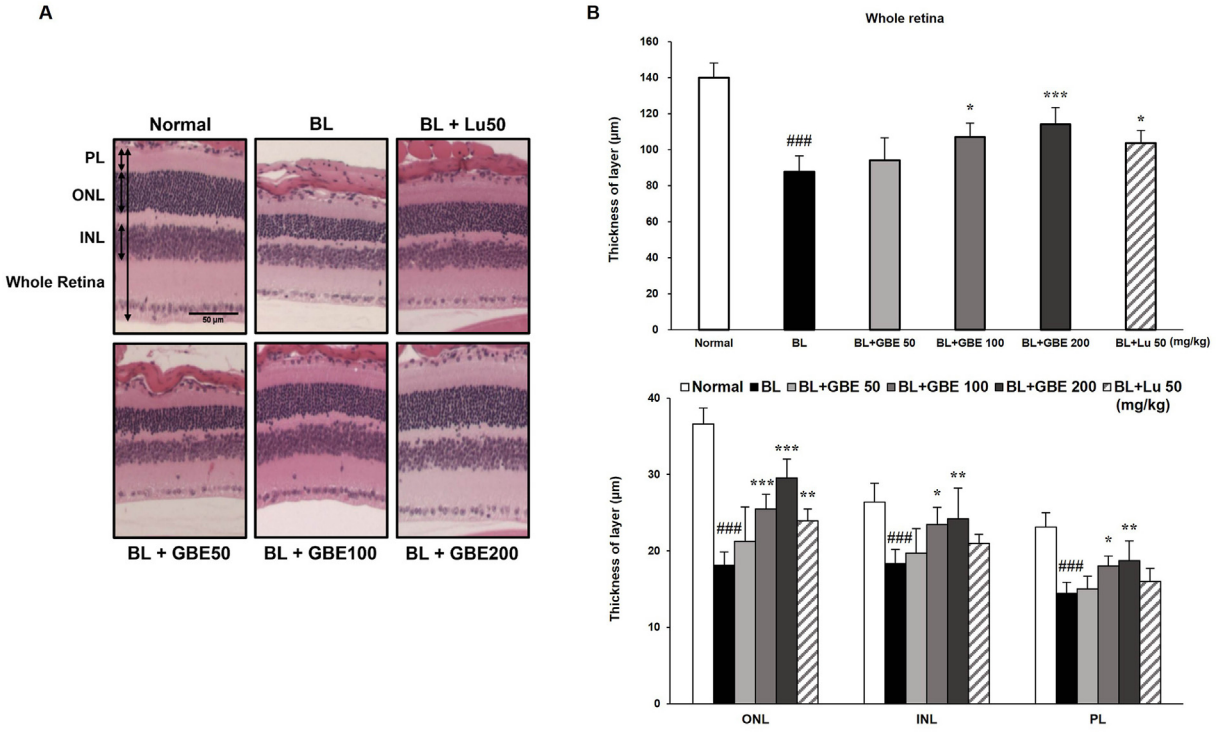

Fig. 4. GBE protects BL induced retinal degeneration in retina. (A) Representative retinal images of H&E staining between 600 μm and 900 μm from the optic nerve. ONL; outer nuclear layer, INL; inner nuclear layer, PL; photoreceptor layer. Scale bar = 50 μm. (B) The thicknesses of whole retina, ONL, INL, and PL were measured at six different locations and averaged. The results were presented as mean ± SD (n = 6), $^{###}p < 0.001$ vs. Normal control group, *p < 0.05, **p < 0.01, ***p < 0.001 vs. Vehicle treated group (BL exposed group).

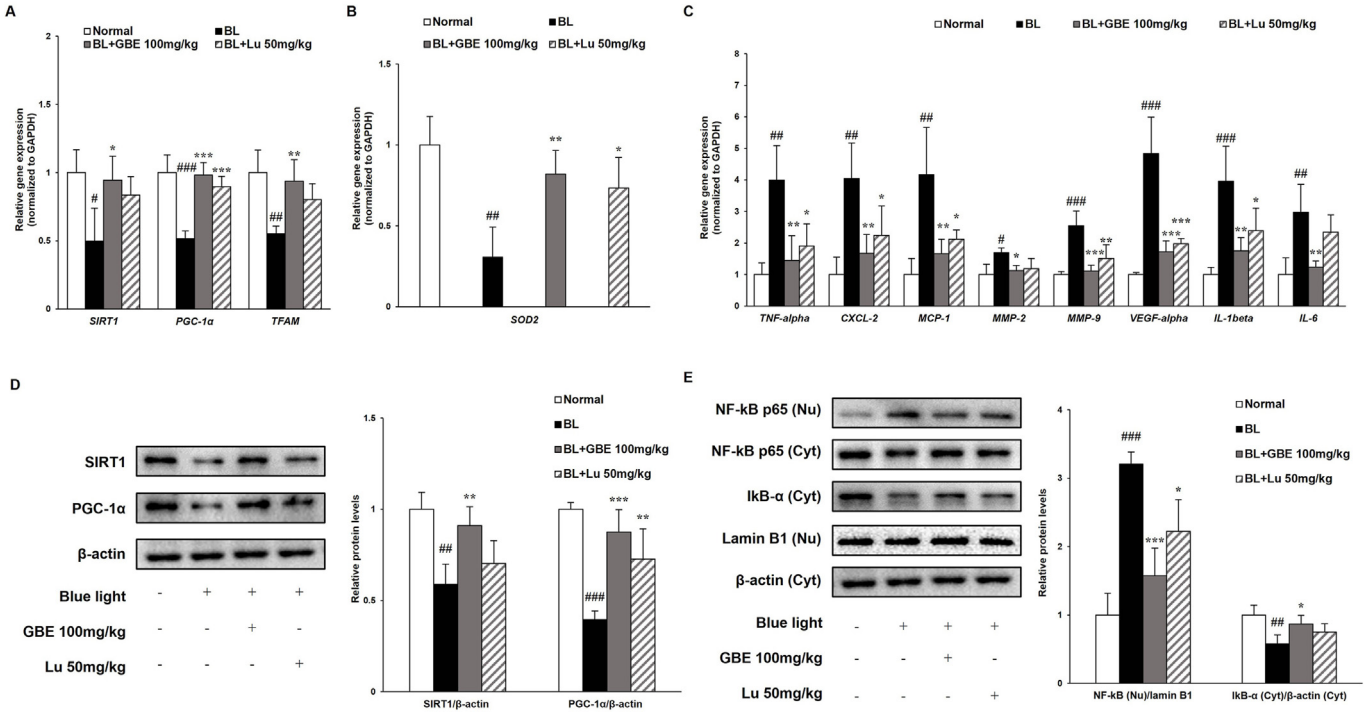

Fig. 5. GBE activates SIRT1/PGC-1α signaling pathway and inhibits BL induced inflammatory response in retina. (A) Gene expressions of *Sirt1, Pgc-1α*, and *Tfam* were analyzed in retina by quantitative real time PCR. (B) Gene expression of *Sod2* was measured using qRT-PCR. (C) Gene expressions of inflammation-related factors (TNF-alpha, CXCL-2, MCP-1, MMP-2, MMP-9, VEGF-alpha, IL-1beta, and IL-6) were measured by qRT-PCR and normalized to GAPDH. (D) Protein levels of SIRT1 (120 kDa) and PGC-1α (92 kDa) were analyzed by western immunoblotting and quantified by band density. (E) Protein levels of NF-kB p65 (65 kDa) and IkBα (37 kDa) were detected using western immunoblotting and quantified by band density. The results were presented as mean ± SD (n = 4) of three independent experiments. $^{#}p < 0.05$, $^{##}p < 0.01$, $^{###}p < 0.001$ vs. Normal control group, *p < 0.05, **p < 0.01, ***p < 0.001 vs. Vehicle treated group (BL exposed group).

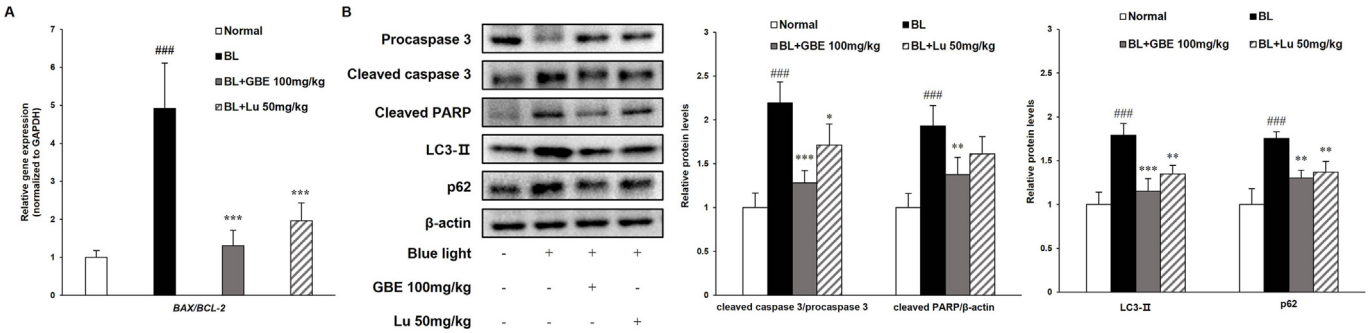

Fig. 6. GBE inhibits apoptosis and restores the inhibition of autophagic flux induced by BL exposure in the retina. (A) Gene expressions of apoptosis-related factors (BAX/BCL-2) were analyzed in retina using qRT-PCR and normalized to GAPDH. (B) Protein levels of procaspase 3 (35 kDa), cleaved caspase 3 (17 kDa), cleaved PARP (89 kDa), LC3-II (14 kDa), and p62 (62 kDa) were measured by western immunoblotting and quantified by band density. The results were presented as mean ± SD (n = 4) of three independent experiments. ###p < 0.001 vs. Normal control group, *p < 0.05, **p < 0.01, ***p < 0.001 vs. Vehicle treated group (BL exposed group).

both pre-and post-treatment systems, ginsenoside Re suppressed BL-induced cell death concentration-dependently (Supplementary Fig. S3). Molecular weight of ginsenoside Re is 947.2. Therefore, 4 μg/mL is converted to about 4 μM according to the molecular weight of ginsenoside Re. Ginsenoside Re, which is contained 5% in GBE, at 4 μM (= 4 μg/mL), exerted similar protective effects with GBE at 40 μg/mL concentration in the pre-and post-treatment systems (Fig. 1D and E and Supplementary Fig. S3). Therefore, we suggest that ginsenoside Re is one of the major active components of GBE.

4. Conclusions

This study aimed to elucidate whether GBE exerted protective effects against BL-induced retinal damage and identify its underlying mechanisms *in vitro* and *in vivo*. GBE prevented BL-induced RPE cell death in a concentration-dependent manner. GBE inhibited inflammation via SIRT1/PGC-1α and NF-kB pathways in RPE cells. GBE also suppressed apoptosis by regulating caspase 3 activation, PARP cleavage, and autophagic flux. Administration of GBE protected the retinal layers (ONL, INL, and PL) against BL-induced retinal degeneration by restoring their thickness. GBE downregulated the expressions of genes and proteins related to inflammation and apoptosis in the retina. Ginsenoside Re, the most abundant component in GBE, is an active ingredient of GBE on retinal degeneration. Therefore, GBE could be a potential agent to prevent dry AMD and progression to wet AMD.

Declaration of competing interest

All authors declare no conflicts of interest.

Appendix A. Supplementary data

Supplementary data to this article can be found online at https://doi.org/10.1016/j.jgr.2022.04.002.

References

[1] Pennington KL, DeAngelis MM. Epidemiology of age-related macular degeneration (AMD): associations with cardiovascular disease phenotypes and lipid factors. Eye Vision 2016;3:1–20.
[2] Kuno N, Fujii S. Dry age-related macular degeneration: recent progress of therapeutic approaches. Curr Mol Pharmacol 2011;4:196–232.
[3] Bressler NM, Bressler SB, Fine SL. Age-related macular degeneration. Surv Ophthalmol 1988;32:375–413.
[4] Grossniklaus HE, Green WR. Choroidal neovascularization. Am J Ophthalmol 2004;137:496–503.
[5] Kauppinen A, Niskanen H, Suuronen T, Kinnunen K, Salminen A, Kaarniranta K. Oxidative stress activates NLRP3 inflammasomes in ARPE-19 cells—implications for age-related macular degeneration (AMD). Immunol Lett 2012;147:29–33.
[6] Kennedy CJ, Rakoczy PE, Constable IJ. Lipofuscin of the retinal pigment epithelium: a review. Eye 1995;9:763–71.
[7] Sparrow JR, Fishkin N, Zhou J, Cai B, Jang YP, Krane S, Itagaki Y, Nakanishi K. A2E, a byproduct of the visual cycle. Vis Res 2003;43:2983–90.
[8] Sparrow JR, Nakanishi K, Parish CA. The lipofuscin fluorophore A2E mediates blue light–induced damage to retinal pigmented epithelial cells. Invest Ophthalmol Vis Sci 2000;41:1981–9.
[9] Jang YP, Matsuda H, Itagaki Y, Nakanishi K, Sparrow JR. Characterization of peroxy-A2E and furan-A2E photooxidation products and detection in human and mouse retinal pigment epithelial cell lipofuscin. J Biol Chem 2005;280:39732–9.
[10] Arnault E, Barrau C, Nanteau C, Gondouin P, Bigot K, Viénot F, Gutman E, Fontaine V, Villette T, Cohen-Tannoudji D. Phototoxic action spectrum on a retinal pigment epithelium model of age-related macular degeneration exposed to sunlight normalized conditions. PLoS One 2013;8:e71398.
[11] Lambert NG, ElShelmani H, Singh MK, Mansergh FC, Wride MA, Padilla M, Keegan D, Hogg RE, Ambati BK. Risk factors and biomarkers of age-related macular degeneration. Prog Retin Eye Res 2016;54:64–102.
[12] Shang Y-M, Wang G-S, Sliney D, Yang C-H, Lee L-L. White light–emitting diodes (LEDs) at domestic lighting levels and retinal injury in a rat model. Environ Health Perspect 2014;122:269–76.
[13] Suzuki M, Tsujikawa M, Itabe H, Du Z-J, Xie P, Matsumura N, Fu X, Zhang R, Sonoda K-h, Egashira K. Chronic photo-oxidative stress and subsequent MCP-1 activation as causative factors for age-related macular degeneration. J Cell Sci 2012;125:2407–15.
[14] Nakamura M, Kuse Y, Tsuruma K, Shimazawa M, Hara H. The involvement of the oxidative stress in murine blue LED light-induced retinal damage model. Biol Pharm Bull 2017;40:1219–25.
[15] Attele AS, Wu JA, Yuan C-S. Ginseng pharmacology: multiple constituents and multiple actions. Biochem Pharmacol 1999;58:1685–93.
[16] Kim J, Cho SY, Kim SH, Kim S, Park C-W, Cho D, Seo DB, Shin SS. Ginseng berry and its biological effects as a natural phytochemical. Natural Products Chemistry & Research; 2016.
[17] Kim C-K, Cho DH, Lee K-S, Lee D-K, Park C-W, Kim WG, Lee SJ, Ha K-S, Goo Taeg O, Kwon Y-G. Ginseng berry extract prevents atherogenesis via anti-inflammatory action by upregulating phase II gene expression. Evid base Compl Alternative Med 2012;2012.
[18] Kuo Y-H, Ikegami F, Lambein F. Neuroactive and other free amino acids in seed and young plants of Panax ginseng. Phytochemistry 2003;62:1087–91.
[19] Wang W, Zhao Y, Rayburn ER, Hill DL, Wang H, Zhang R. In vitro anti-cancer activity and structure–activity relationships of natural products isolated from fruits of Panax ginseng. Cancer Chemother Pharmacol 2007;59:589–601.
[20] Lee SY, Kim YK, Park NI, Kim CS, Lee CY, Park SU. Chemical constituents and biological activities of the berry of Panax ginseng. J Med Plants Res 2010;4:349–53.
[21] Chung I-M, Lim J-J, Ahn M-S, Jeong H-N, An T-J, Kim S-H. Comparative phenolic compound profiles and antioxidative activity of the fruit, leaves, and roots of Korean ginseng (Panax ginseng Meyer) according to cultivation years. J Ginseng Res 2016;40:68–75.
[22] Pérez ZEJ, Ramya Mathiyalagan JM, Kim Y-J, Kang HM, Abbai R, Seo KH, Wang D, Soshnikova V, Yang DC. Ginseng-berry-mediated gold and silver nanoparticle synthesis and evaluation of their in vitro antioxidant, antimicrobial, and cytotoxicity effects on human dermal fibroblast and murine melanoma skin cell lines. Int J Nanomed 2017;12:709.
[23] Li KR, Zhang ZQ, Yao J, Zhao YX, Duan J, Cao C, Jiang Q. Ginsenoside Rg-1 protects retinal pigment epithelium (RPE) cells from cobalt chloride (CoCl2) and hypoxia assaults. PLoS One 2013;8:e84171.

[24] Bian M, Du X, Wang P, Cui J, Xu J, Gu J, Zhang T, Chen Y. Combination of ginsenoside Rb1 and Rd protects the retina against bright light-induced degeneration. Sci Rep 2017;7:6015.
[25] Lee BL, Kang JH, Kim HM, Jeong SH, Jang DS, Jang YP, Choung SY. Polyphenol-enriched Vaccinium uliginosum L. fractions reduce retinal damage induced by blue light in A2E-laden ARPE19 cell cultures and mice. Nutr Res (NY) 2016;36:1402–14.
[26] Lee MY, Seo HS, Singh D, Lee SJ, Lee CH. Unraveling dynamic metabolomes underlying different maturation stages of berries harvested from Panax ginseng. J Ginseng Res 2020;44:413–23.
[27] Joo K-M, Lee J-H, Jeon H-Y, Park C-W, Hong D-K, Jeong H-J, Lee SJ, Lee S-Y, Lim K-M. Pharmacokinetic study of ginsenoside Re with pure ginsenoside Re and ginseng berry extracts in mouse using ultra performance liquid chromatography/mass spectrometric method. J Pharmaceut Biomed Anal 2010;51:278–83.
[28] Kim J, Cho K, Choung SY. Protective effect of Prunella vulgaris var. L extract against blue light induced damages in ARPE-19 cells and mouse retina. Free Radic Biol Med 2020;152:622–31.
[29] Kaarniranta K, Kajdanek J, Morawiec J, Pawlowska E, Blasiak J. PGC-1α protects RPE cells of the aging retina against oxidative stress-induced degeneration through the regulation of senescence and mitochondrial quality control. The significance for AMD pathogenesis. Int J Mol Sci 2018;19.
[30] Yang H, Zhang W, Pan H, Feldser HG, Lainez E, Miller C, Leung S, Zhong Z, Zhao H, Sweitzer S, et al. SIRT1 activators suppress inflammatory responses through promotion of p65 deacetylation and inhibition of NF-κB activity. PLoS One 2012;7:e46364.
[31] Santos L, Escande C, Denicola A. Potential modulation of sirtuins by oxidative stress. Oxid Med Cell Longev 2016;2016:9831825.
[32] Saadat KA, Murakami Y, Tan X, Nomura Y, Yasukawa T, Okada E, Ikeda Y, Yanagi Y. Inhibition of autophagy induces retinal pigment epithelial cell damage by the lipofuscin fluorophore A2E. FEBS Open Bio 2014;4:1007–14.
[33] Yamamoto Y, Gaynor RB. Role of the NF-kB pathway in the pathogenesis of human disease states. Curr Mol Med 2001;1:287–96.
[34] Suárez-Barrio C, Del Olmo-Aguado S, García-Pérez E, Fernández-Vega-Cueto L, Fernández-Vega Cueto A, Baamonde-Arbaiza B, Fernández-Vega L, Merayo-Lloves J. Plasma rich in growth factors promotes autophagy in ARPE19 cells in response to oxidative stress induced by blue light. Biomolecules 2021:11.
[35] Okamoto T, Ozawa Y, Kamoshita M, Osada H, Toda E, Kurihara T, Nagai N, Umezawa K, Tsubota K. The neuroprotective effect of rapamycin as a modulator of the mTOR-NF-κB Axis during retinal inflammation. PLoS One 2016;11:e0146517.
[36] Jürgensmeier JM, Xie Z, Deveraux Q, Ellerby L, Bredesen D, Reed JC. Bax directly induces release of cytochrome c from isolated mitochondria. Proc Natl Acad Sci Unit States Am 1998;95:4997–5002.
[37] Chaitanya GV, Steven AJ, Babu PP. PARP-1 cleavage fragments: signatures of cell-death proteases in neurodegeneration. Cell Commun Signal : CCS 2010;8:31.
[38] Jeong SY, Gu X, Jeong KW. Photoactivation of N-retinylidene-N-retinylethanolamine compromises autophagy in retinal pigmented epithelial cells. Food Chem Toxicol 2019;131:110555.
[39] Kaarniranta K, Tokarz P, Koskela A, Paterno J, Blasiak J. Autophagy regulates death of retinal pigment epithelium cells in age-related macular degeneration. Cell Biol Toxicol 2017;33:113–28.
[40] Liu J, Copland DA, Theodoropoulou S, Chiu HA, Barba MD, Mak KW, Mack M, Nicholson LB, Dick AD. Impairing autophagy in retinal pigment epithelium leads to inflammasome activation and enhanced macrophage-mediated angiogenesis. Sci Rep 2016;6:20639.
[41] Mitter SK, Song C, Qi X, Mao H, Rao H, Akin D, Lewin A, Grant M, Dunn Jr W, Ding J. Dysregulated autophagy in the RPE is associated with increased susceptibility to oxidative stress and AMD. Autophagy 2014;10:1989–2005.
[42] Xia H, Hu Q, Li L, Tang X, Zou J, Huang L, Li X. Protective effects of autophagy against blue light-induced retinal degeneration in aged mice. Sci China Life Sci 2019;62:244–56.
[43] Ma L, Lin XM. Effects of lutein and zeaxanthin on aspects of eye health. J Sci Food Agric 2010;90:2–12.